TEKA. COMMISSION OF MOTORIZATION AND ENERGETICS IN AGRICULTURE – 2012, Vol. 12, No. 2, 279–283

Pressure distributions in oil film in the front gap of a hydrostatic thrust bearing

Tadeusz Zloto, Konrad Kowalski

Institute of Mechanical Technologies
Czestochowa University of Technology

Summary. The paper presents pressure distributions in oil film in a front variable-height gap of a hydrostatic thrust bearing. On the basis of the Navier-Stokes equations and the continuity equation a formula was found describing the pressure in the gap. The influence was analyzed of geometrical dimensions and exploitation parameters of thrust bearings on circumferential pressure distribution near the smallest gap height. The numerical results of pressure values take into account the effects of oil viscosity, the smallest gap height, the inclination angle and angular velocity of the upper wall of the bearing, the pressure feeding the bearing and the ratio of the external to the internal bearing radius.

Key words: hydrostatic thrust bearing, pressure distributions, front gap.

INTRODUCTION

Hydrostatic thrust bearings support load distributed axially with respect to the shaft. Processes occurring in hydrostatic thrust bearings depend on the kind of gap. Typically, the front gap height is variable [13,20]. The gap shape can be confusor, diffuser or parallel and the pressure distribution varies accordingly (Fig.1) [9].

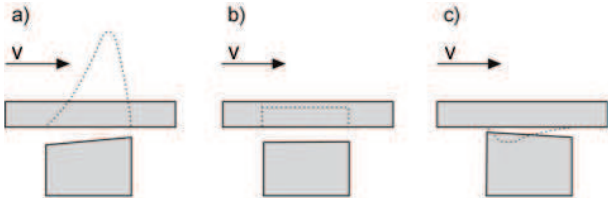

Fig. 1. Pressure distributions in the front gap: a) confusor, b) parallel, c) diffuser [9]

The operation of the valve plate - cylinder block system or of the slipper - swashplate system in an axial pump is analogous to the operation of a hydrostatic thrust bearing [6,7].

Complex phenomena occurring in gaps of hydrostatic bearings affect the efficiency of hydraulic machines [1,2,5,7,11,12,15,16,17,18,19] and devices and are therefore in the centre of interest of designers and development units.

Fig. 2 presents a general diagram of a hydrostatic thrust bearing with the front variable-height gap. The upper wall rotates with the angular velocity ω around its axis and is typically inclined by the angle ε with respect to the lower wall. Oil flows out of the central chamber of the upper wall to the outside of the gap.

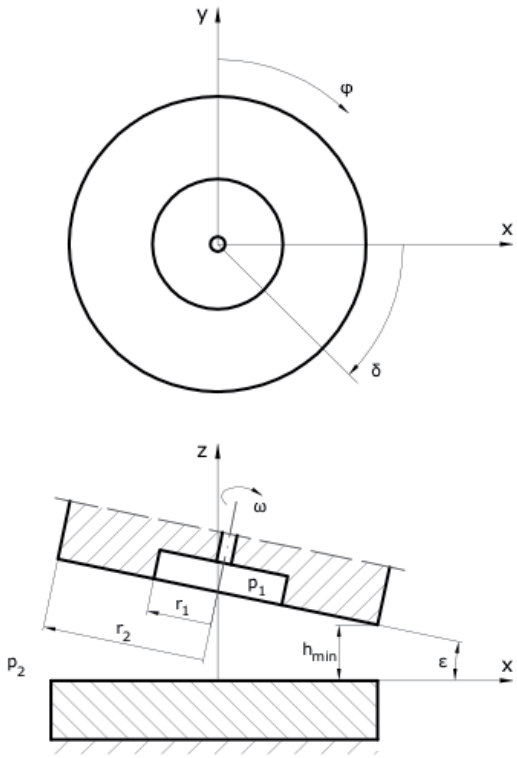

Fig. 2. Hydrostatic thrust bearing with a front variable-height gap

In a confusor gap an over- pressure peak occurs next to the smallest gap height whereas in a diffuser gap there is negative pressure limited by cavitation, which complicates the analytical description of the phenomenon. Cavitation also results in damages to the material in the form of crevasses [10].

APPLICATION OF THE NAVIER-STOKES EQUATIONS FOR DETERMINING OIL PRESSURE DISTRIBUTIONS IN A FRONT GAP

Pressure changes in the front gap can be described on the basis of the Navier-Stokes equations and the flow continuity equation represented in the cylindrical coordinate system r, φ, z [3,4,8,14,21]:

$$\frac{\partial \mathrm{v}_r}{\partial t}+\mathrm{v}_r\frac{\partial \mathrm{v}_r}{\partial r}+\frac{\mathrm{v}_\varphi}{r}\frac{\partial \mathrm{v}_r}{\partial \varphi}+\mathrm{v}_z\frac{\partial \mathrm{v}_r}{\partial z}-\frac{\mathrm{v}_\varphi^{\,2}}{r}=$$
$$=\nu\left(\frac{\partial^2 \mathrm{v}_r}{\partial r^2}+\frac{1}{r}\frac{\partial \mathrm{v}_r}{\partial r}+\frac{1}{r^2}\frac{\partial^2 \mathrm{v}_r}{\partial \varphi^2}+\frac{\partial^2 \mathrm{v}_r}{\partial z^2}-\frac{\mathrm{v}_r}{r^2}-\frac{2}{r^2}\frac{\partial \mathrm{v}_\varphi}{\partial \varphi}\right)-\frac{1}{\rho}\frac{\partial p}{\partial r},\quad(1)$$

$$\frac{\partial \mathrm{v}_\varphi}{\partial t}+\mathrm{v}_r\frac{\partial \mathrm{v}_\varphi}{\partial r}+\frac{\mathrm{v}_\varphi}{r}\frac{\partial \mathrm{v}_\varphi}{\partial \varphi}+\mathrm{v}_z\frac{\partial \mathrm{v}_\varphi}{\partial z}+\frac{2\mathrm{v}_r\mathrm{v}_\varphi}{r}=$$
$$=\nu\left(\frac{\partial^2 \mathrm{v}_\varphi}{\partial r^2}+\frac{1}{r}\frac{\partial \mathrm{v}_\varphi}{\partial r}+\frac{1}{r^2}\frac{\partial^2 \mathrm{v}_\varphi}{\partial \varphi^2}+\frac{\partial^2 \mathrm{v}_\varphi}{\partial z^2}+\frac{2}{r^2}\frac{\partial \mathrm{v}_r}{\partial \varphi}-\frac{\mathrm{v}_\varphi}{r^2}\right)-\frac{1}{\rho r}\frac{\partial p}{\partial \varphi},\quad(2)$$

$$\frac{\partial \mathrm{v}_z}{\partial t}+\mathrm{v}_r\frac{\partial \mathrm{v}_z}{\partial r}+\frac{\mathrm{v}_\varphi}{r}\frac{\partial \mathrm{v}_z}{\partial \varphi}+\mathrm{v}_z\frac{\partial \mathrm{v}_z}{\partial z}=$$
$$=\nu\left(\frac{\partial^2 \mathrm{v}_z}{\partial r^2}+\frac{1}{r}\frac{\partial \mathrm{v}_z}{\partial r}+\frac{1}{r^2}\frac{\partial^2 \mathrm{v}_z}{\partial \varphi^2}+\frac{\partial^2 \mathrm{v}_z}{\partial z^2}\right)-\frac{1}{\rho}\frac{\partial p}{\partial z},\quad(3)$$

$$\frac{\partial \mathrm{v}_r}{\partial r}+\frac{1}{r}\frac{\partial \mathrm{v}_\varphi}{\partial \varphi}+\frac{\partial \mathrm{v}_z}{\partial z}+\frac{\mathrm{v}_r}{r}=0.\quad(4)$$

It was assumed that oil is incompressible, the flow is laminar and isothermal, liquid motion is steady and uniform. The gap is completely filled with oil and tangent stress is Newtonian. Liquid particles directly adjacent to the moving surface retain their velocity. Besides, the surfaces limiting the gap are rigid and inertia forces are negligible. If $\mathrm{v}_r = \mathrm{v}_r(r, z)$ and $\mathrm{v}_z = 0$, Eqs. (1 ÷ 4) become:

$$0=\nu\frac{\partial^2 \mathrm{v}_r}{\partial z^2}-\frac{1}{\rho}\frac{\partial p}{\partial r},\quad(5)$$

$$0=\frac{\partial^2 \mathrm{v}_\varphi}{\partial z^2},\quad(6)$$

$$0=\frac{\partial p}{\partial z},\quad(7)$$

$$0=\frac{\partial \mathrm{v}_r}{\partial r}+\frac{1}{r}\frac{\partial \mathrm{v}_\varphi}{\partial \varphi}+\frac{\mathrm{v}_r}{r}.\quad(8)$$

Introducing the dynamic viscosity coefficient $\mu = \nu\rho$ turns Eq. (5) into

$$\frac{\partial^2 \mathrm{v}_r}{\partial z^2}=\frac{1}{\mu}\frac{\partial p}{\partial r}.\quad(9)$$

After double integrating Eq. (9) becomes:

$$\mathrm{v}_r=\frac{1}{2\mu}\frac{\partial p}{\partial r}z^2+C_1z+C_2.\quad(10)$$

The integration constants C_1 and C_2 are determined on the basis of the following boundary conditions:

$$\text{for z = 0, } \mathrm{v}_r = 0 \text{ and for z = h, } \mathrm{v}_r = 0,$$

The integration constants are, respectively:

$$C_1=-\frac{1}{2\mu}\frac{\partial p}{\partial r}h,\quad(11)$$

$$C_2 = 0.\quad(12)$$

Substituting (11) and (12) into Eq. (10):

$$\mathrm{v}_r=\frac{1}{2\mu}\frac{\partial p}{\partial r}\left(z^2-hz\right).\quad(13)$$

After integrating Eq. (6) twice with respect to the variable z:

$$\mathrm{v}_\varphi=C_3z+C_4.\quad(14)$$

The integration constants C_3 and C_4 are obtained on the basis of the following boundary conditions

$$\text{for z = 0, } \mathrm{v}_\varphi = 0 \text{ and for z = h, } \mathrm{v}_\varphi = \omega\cdot r,$$

The integrations constants are, respectively:

$$C_3=\frac{\omega r}{h},\quad(15)$$

$$C_4 = 0.\quad(16)$$

Substituting the constants C_3 and C_4 into Eq. (14) leads to:

$$\mathrm{v}_\varphi=\frac{\omega r}{h}z.\quad(17)$$

When (13) and (17) are taken into account, Eq. (8) becomes:

$$0=\frac{1}{2\mu}\frac{\partial^2 p}{\partial r^2}\left(z^2-hz\right)-\omega z\frac{1}{h^2}\frac{dh}{d\varphi}+\frac{1}{2\mu r}\frac{\partial p}{\partial r}\left(z^2-hz\right).\quad(18)$$

After integrating Eq. (18) with respect to the variable z within the limits from 0 to h and with subsequent transformations:

$$\frac{\partial}{\partial r}\left(r\frac{\partial p}{\partial r}\right)=-6\mu\omega r\frac{1}{h^3}\frac{dh}{d\varphi}.\quad(19)$$

Then, integrating Eq. (19) twice with respect to the variable r

$$p = -\frac{3}{2}\mu\omega r^2 \frac{1}{h^3}\frac{dh}{d\varphi} + C_5 \ln r + C_6 \tag{20}$$

The integration constants C_5 and C_6 are obtained on the basis of the following boundary conditions

for r = r_1, p = p_1 and for r = r_2, p = p_2 = 0

The integration constants are, respectively

$$C_5 = \frac{3}{2}\mu\omega \frac{1}{\ln\frac{r_2}{r_1}}\frac{1}{h^3}\frac{dh}{d\varphi}\left(r_2^2 - r_1^2\right) - \frac{p_1}{\ln\frac{r_2}{r_1}} \tag{21}$$

$$C_6 = \frac{3}{2}\mu\omega r_2^2 \frac{1}{h^3}\frac{dh}{d\varphi} - \frac{3}{2}\mu\omega \frac{\ln r_2}{\ln\frac{r_2}{r_1}}\frac{1}{h^3}\frac{dh}{d\varphi}\left(r_2^2 - r_1^2\right) + \frac{p_1 \ln r_2}{\ln\frac{r_2}{r_1}} \tag{22}$$

Substituting the integration constants C_5 and C_6 to Eq. (20) leads to the following formula for the pressure p in the front gap

$$p = \frac{3}{2}\mu\omega \frac{1}{\ln\frac{r_2}{r_1}}\frac{1}{h^3}\frac{dh}{d\varphi}\left[\left(r_2^2 - r^2\right)\ln\frac{r_2}{r_1} - \left(r_2^2 - r_1^2\right)\ln\frac{r_2}{r}\right] + p_1 \frac{\ln\frac{r_2}{r}}{\ln\frac{r_2}{r_1}} \tag{23}$$

RESULTS OF SIMULATION EXPERIMENTS ON PRESURE DISTRIBUTION NEXT TO THE SMALLEST HEIGHT OF THE FRONT GAP

The simulation experiments were carried out by means of software. The gap height was obtained from [22]

$$h = -r\sin\varphi\cos\delta\tan\varepsilon - r\cos\varphi\sin\delta\tan\varepsilon + r_2\tan\varepsilon + h_1 \tag{24}$$

The following parameters were assumed in the computations:

- pressure at the gap entrance p_1 = 20 [MPa],
- pressure at the gap exit p_2 = 0 [MPa],
- bearing internal radius r_1 = 0.004 [m] and bearing external radius r_2 = 0.012 [m],
- dynamic viscosity coefficient μ within the range 0.0122 - 0.0616 [Pas],
- angular velocity ω of the upper wall within the range 100 - 200 [rad/s],
- inclination angle ε of the upper wall within the range 0.01 - 0.03 [º],
- angle δ = 45 [º] of the smallest gap height h_1 with respect to the axis x.

Fig. 3 presents the circumferential pressure distribution on the radius r = 0.011 [m] next to the smallest front gap height. As the smallest gap is approached along the circumference in a confusor gap, an over-pressure peak is encountered. At the other side, when moving away from the smallest gap a negative pressure occurs, limited by cavitation.

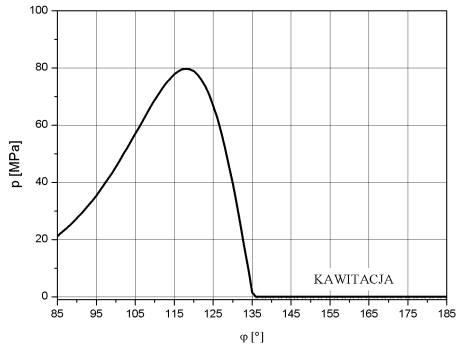

Fig. 3. Distribution of circumferential oil pressure next to the smallest gap height on the radius r = 0.011 [m] (ε = 0.02 [º], h_1 = 0.5 [μm], μ = 0.0253 [Pas], ω = 150 [rad/s], p_1 = 20 [MPa], r_2/r_1 = 3)

Fig. 4 presents oil pressure distributions in a confusor gap of a thrust bearing depending on the inclination angle of the upper wall. As the angle decreases, the maximum pressure increases.

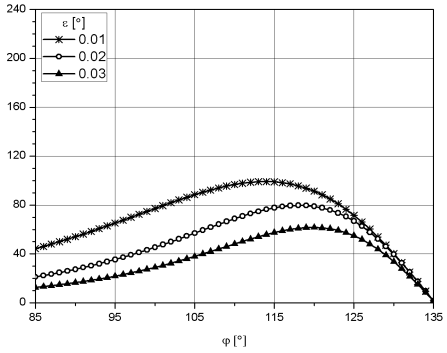

Fig. 4. Distributions of circumferential oil pressure on the radius r = 0.011 [m] in a confusor gap depending on the angle ε of the upper wall inclination (h_1 = 0.5 [μm], μ = 0.0253 [Pas], ω = 150 [rad/s], p_1 = 20 [MPa], $r_2 r_1$ = 3)

Fig. 5 presents oil pressure distributions in a confusor gap of a thrust bearing depending on the smallest gap height. Similarly as above, as the minimum gap height decreases, the maximum pressure increases.

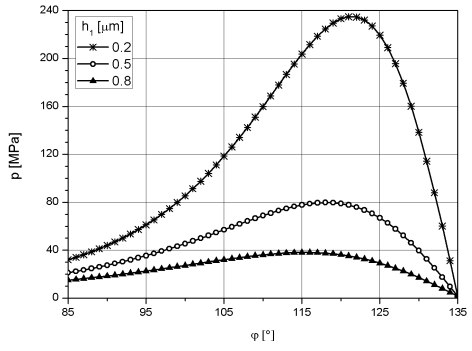

Fig. 5. Oil pressure distributions on the radius r = 0.011 [m] in a front confusor gap depending on the smallest gap height h_1 (ε = 0.02 [º], μ = 0.0253 [Pas], ω = 150 [rad/s], p_1 = 20 [MPa], $r_2 r_1$ = 3)

Fig. 6 shows oil pressure distributions in a confusor gap of a thrust bearing depending on oil viscosity. With increase in oil viscosity, the maximum pressure also increases.

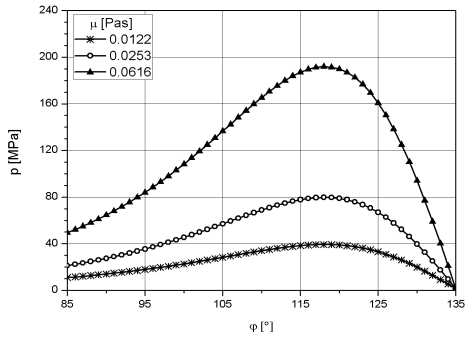

Fig. 6. Distributions of circumferential oil pressure on the radius $r = 0.011$ [m] in a front confusor gap depending on the oil viscosity coefficient μ ($\varepsilon = 0.02$ [º], $h_1 = 0.5$ [μm], $\omega = 150$ [rad/s], $p_1 = 20$ [MPa], $r_2 r_1 = 3$)

In Fig. 7 oil pressure distributions can be seen in a confusor gap of a thrust bearing depending on the angular velocity of the bearing upper wall. As the angular velocity increases, the maximum pressure increases too.

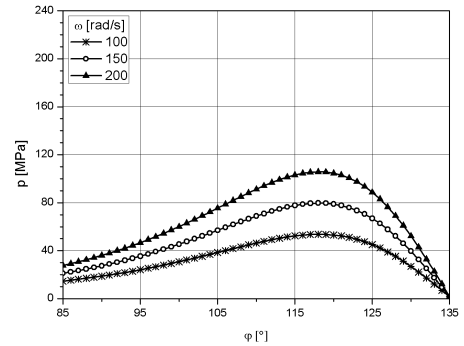

Fig. 7. Distributions of circumferential oil pressure on the radius $r = 0.011$ [m] in a front confusor gap depending on the angular velocity ω of the upper wall ($\varepsilon = 0.02$ [º], $h_1 = 0.5$ [μm], $\mu = 0.0253$ [Pas], $p_1 = 20$ [MPa], $r_2 r_1 = 3$)

Fig. 8 presents oil pressure distributions in a confusor gap of a thrust bearing depending on the pressure feeding the bearing. It can be observed that the influence of the feeding pressure on the maximum pressure value is small.

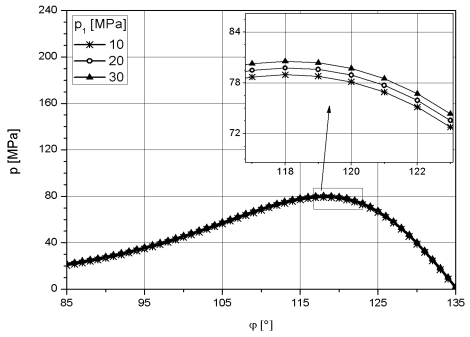

Fig. 8. Distributions of circumferential oil pressure on the radius $r = 0.011$ [m] in a front confusor gap depending on the feeding pressure p_1 of a thrust bearing ($\varepsilon = 0.02$ [º], $h_1 = 0.5$ [μm], $\mu = 0.0253$ [Pas], $\omega = 150$ [rad/s], $r_2 r_1 = 3$)

Fig. 9 shows distributions of oil hyper-pressure in a confusor gap of a thrust bearing depending on the ratio of the external to internal bearing radius. As the ratio increases, the maximum pressure in the gap also increases.

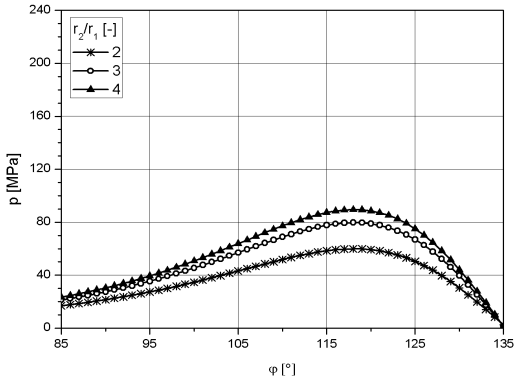

Fig. 9. Distributions of circumferential oil pressure on the radius $r = 0.011$ [m] in a front confusor gap depending on the bearing dimensions ($\varepsilon = 0.02$ [º], $h_1 = 0.5$ [μm], $\mu = 0.0253$ [Pas], $\omega = 150$ [rad/s], $p_1 = 20$ [MPa])

CONCLUSIONS

The study leads to the following conclusions:

1. The computation model adopted in this paper enables determining pressure distributions in front gaps of hydrostatic thrust bearings.
2. The occurrence of pressure peaks in a front confusor gap depends on a number of geometrical and exploitation parameters of the thrust bearing.
3. A local increase of pressure in a front confusor gap can contribute to additional relief of the hydrostatic thrust bearing, whereas a pressure drop in a front diffuser gap is disadvantageous, since it causes cavitation and, consequently, material damage.

REFERENCES

1. **Baszta T. M.:** Hydraulika w budowie maszyn. Poradnik. WNT, Warszawa 1966.
2. **Baszta T. M.:** Maszinostroitielnaja gidrawlika. Maszinostrojenie, Moskwa 1971.
3. **Bukowski J.:** Mechanika płynów. PWN, Warszawa 1975.
4. **Fuller D. D.:** Theory and practice of lubrication for engineers. John Wiley and Sons Inc, New York 1966.
5. **Hama T., Kurisu K., Matsushima K., Fujimoto H., Takuda H.:** Outflow Characteristics of a Pressure Medium during Sheet Hydroforming, ISIJ International, Vol. 49, No. 2/2009, 239-246.
6. **Ivantysyn J., Ivantysynova M.:** Hydrostatic Pumps and Motors. Academia Books International, New Delhi 2001.
7. **Ivantysynova M.:** Design and Modeling of Fluid Power Systems. Purdue University 2009.

8. **Kondakow L. A.:** Uszczelnienia układów hydraulicznych. WNT, Warszawa 1975.
9. **Jang D. S.:** Verlustanalise an Axialkolbeneinheiten. Dissertation RWTH, Aachen 1997.
10. **Kunze T., Brunner H.:** Vibroakustische und optische Untersuchung der Kavitation bei Axialkolbenmaschinen. Ölhydraulik und Pneumatik, Nr 8/1996, 542-546.
11. **Lasaar R.:** The Influence of the Microscopic and Macroscopic Gap Geometry on the Energy Dissipation in the Lubricating Gaps of Displacement Machines. Proc. of 1-st FPNI-PhD Symposium, Hamburg 2000.
12. **Murrenhoff H.:** Grundlagen der Fluidtechnik. Teil 1: Hydraulik, Shaker Verlag, Aachen 2005.
13. **Osiecki A.:** Hydrostatyczny napęd maszyn. WNT, Warszawa 2004.
14. **Osipow A. F.:** Objemnyje gidrowliczieskie masziny. Maszinostrojenie, Moskwa 1966.
15. **Podolski M. E., 1981:** Upornyje podszipniki skolżenia. Leningrad 1981.
16. **Ryzhakov A., Nikolenko I., Dreszer K., 2009:** Selection of discretely adjustable pump parameters for hydrualic druves of mobile equipment. Polska Akademia Nauk, Teka Komisji Motoryzacji i Energetyki Rolnictwa. Tom IX, 267-276, Lublin.
17. **Stryczek S.:** Napęd hydrostatyczny. Elementy i układy. WNT, Warszawa 1984.
18. **Szydelski Z., Olechowicz J.:** Elementy napędu i sterowania hydraulicznego i pneumatycznego. PWN, Warszawa 1986.
19. **Tajanowskij G., Tanas W., 2011:** Dynamic potential of passableness of the agricultural traction-transport technological machine with a hydrodrive of wheels. Polska Akademia Nauk, Teka Komisji Motoryzacji i Energetyki Rolnictwa. Tom XIC, 306-319, Lublin.
20. **Trifonow O. N.:** Gidrawliczieskie sistemy mietałoriežuszczych stankow. MSI, Moskwa 1974.
21. **Walczak J.:** Inżynierska mechanika płynów. WNT, Warszawa 2010.
22. **Zloto T.:** Modelling the pressure distribution in oil film in the variable height gap between the valve plate and cylinder block in the Arial piston pump. Polska Akademia Nauk, Teka Komisji Motoryzacji i Energetyki Rolnictwa, Vol.V, nr 11/2009, T. IX, 418-430.

ROZKŁADY CIŚNIENIA W FILMIE OLEJOWYM SZCZELINY CZOŁOWEJ ŁOŻYSKA HYDROSTATYCZNEGO WZDŁUŻNEGO

S t r e s z c z e n i e. W artykule przedstawiono rozkłady ciśnienia w filmie olejowym szczeliny czołowej o zmiennej wysokości w łożysku hydrostatycznym wzdłużnym. W oparciu o równania Naviera-Stokesa i równanie ciągłości wyznaczono zależność określającą ciśnienie panujące w szczelinie. W pracy analizowano wpływ parametrów geometryczno-eksploatacyjnych łożysk wzdłużnych na rozkłady ciśnienia obwodowego w otoczeniu najmniejszej wysokości szczeliny. Przedstawiono rezultaty obliczeń wartości ciśnienia z uwzględnieniem wpływu lepkości oleju, najmniejszej wysokości szczeliny, kąta pochylenia i prędkości kątowej górnej ścianki łożyska, ciśnienia zasilającego łożysko oraz ilorazu promienia zewnętrznego i wewnętrznego łożyska.

S ł o w a k l u c z o w e: łożysko hydrostatyczne wzdłużne, rozkłady ciśnienia, szczelina czołowa.